Science of the Total Environment 926 (2024) 171847

Contents lists available at ScienceDirect

Science of the Total Environment

journal homepage: www.elsevier.com/locate/scitotenv

Sustainable application of surfactants in soil remediation: Selective pollutants adsorption and hydrogen peroxide-driven adsorbent regeneration

Andrés Sánchez-Yepes, Aurora Santos, Arturo Romero, David Lorenzo *

Chemical Engineering and Materials Department, Complutense University of Madrid, Spain

HIGHLIGHTS

- Chlorinated organic compounds in emulsion were selectively adsorbed in GAC column.
- Spent GAC was sustainably regenerated using the heterogeneous Fenton reaction.
- 50 % of the initial COCs adsorption capacity was maintained after 5 cycles.
- Surfactant adsorption decreases, and surfactant recovery increases with each cycle.
- The adsorbed iron remained stable in the GAC after four regeneration cycles.

GRAPHICAL ABSTRACT

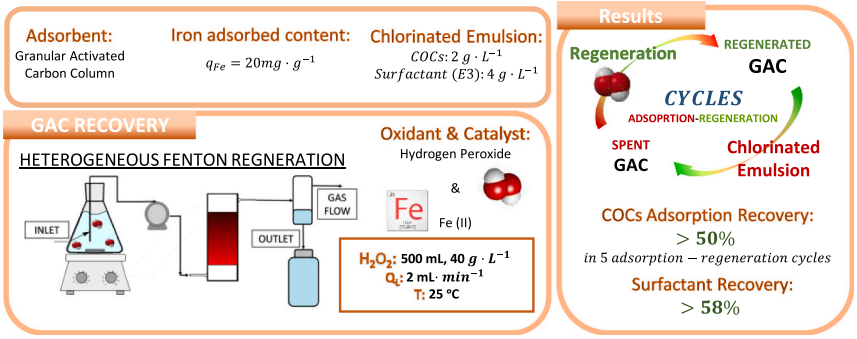

ARTICLE INFO

Keywords:
Adsorption and regeneration cycles
Surfactant
Emulsion
Chlorinated organic compound
Heterogeneous Fenton reaction

ABSTRACT

The uncontrolled disposal of the liquid lindane wastes have led to the formation of dense non-aqueous phase liquids (DNAPL), consisting of 28 chlorinated organic compounds (COCs), contaminating soil and groundwater. Surfactant-enhanced aquifer remediation is proposed as technology to treat these sites. However, the polluted emulsion generated must be manged on-site. In this work a two-step process is applied to treat emulsion composed of *E*-Mulse® 3 (4 g·L^{-1}) as surfactant and a DNAPL (2 g_{COCs}·L^{-1}). In the first, the COCs were selectively adsorbed in a granular activated carbon (GAC) column with Fe (II) previously adsorbed (10–20mg·g-1) onto the carbon surface, recovering an aqueous phase with surfactant for their reuse. In the second step, the spent GAC was regenerated with a 40 g·L^{-1} solution of hydrogen peroxide fed to the column at 2 mL·min^{-1} to promote the oxidation of the COCs adsorbed in the GAC. The kinetic and adsorption model in a multisolute (surfactant and DNAPL) system has been proposed. Five successive cycles of regeneration/adsorption have been successfully applied in the column process. About 50 % of the COCs were retained from the emulsion, and more than 70 % of the surfactant was recovered. The consumption of unproductive oxidants decreased with the number of regeneration cycles. The water effluent obtained after regeneration of GAC did not present chlorinated compounds desorbed and nontoxic by-products generated, such as short-chain acids.

* Corresponding author.
E-mail address: dlorenzo@quim.ucm.es (D. Lorenzo).

https://doi.org/10.1016/j.scitotenv.2024.171847
Received 29 December 2023; Received in revised form 20 February 2024; Accepted 19 March 2024
Available online 23 March 2024

1. Introduction

Bad practices in the disposal of chemical wastes from industrial activity have caused severe environmental problems in many parts of Europe. Large masses of hydrophobic organic compounds (HOCs) were dumped uncontrolled in unprepared landfills, resulting in widespread soil, surface, and groundwater contamination (Panagos et al., 2013). The hydrophobic nature of this HOCs can form a dense non-aqueous liquid phase (DNAPL) (Fernández et al., 2013; Santos et al., 2018; Seyedabbasi et al., 2012). This DNAPL leached through the subsoil and accumulated in the non-permeable layers, contaminating soil and groundwater.u

Traditional approaches to remediation of these soils and groundwater, such as pumping or in-situ chemical oxidation processes, may be limited by the low solubility of HOCs (Siegrist et al., 2011). To overcome this advantage, the injection of aqueous solutions containing surfactants into the subsurface and the subsequent extraction of contaminated emulsions (Huo et al., 2020b; Shams et al., 2021) have raised scientific interest. This method is known as surfactant-enhanced aquifer remediation (SEAR) technology. However, its main drawback is that the soil contaminants are transferred to the emulsion phase, comprised of HOCs and surfactants, that must be managed appropriately (Huo et al., 2020a; Sáez et al., 2022).

The posttreatment of the polluted emulsion generated must be designed from a social, economic, and environmental point of view. In this way, the selective removal of HOCs and recovery of surfactants for their reuse in subsequent SEAR treatments are critical in a large-scale application (Trellu et al., 2021). Selective retention of organic compounds by adsorption on activated carbon is proposed as a cost-effective way to separate pollutants from the emulsion (Ahn et al., 2007; Ahn et al., 2008a; Ahn et al., 2010b; Rosas et al., 2013). Activated carbon is a selective adsorbent where HOCs have a much higher partition coefficient than most non-ionic surfactants used to treat contaminated soils (Ahn et al., 2007; Ahn et al., 2008a). However, this proposal generates a new waste that must be managed appropriately due to the high toxicity of these absorbed compounds.

The recovery of adsorbent materials by oxidation processes is a sustainable alternative. Different oxidants, such as hydrogen peroxide oxidation and persulfate (Huling et al., 2011; Jatta et al., 2019; Peng et al., 2019; Xiao et al., 2020), have been tested. Authors studied the recovery efficiency of spent activated carbons using different molar ratios of hydrogen peroxide and Fe (II) in solution and different contaminates such as limonene or methyl ethyl ketone (Anfruns et al., 2013), chlorinated compounds (Cai et al., 2020; Toledo et al., 2003), biological effluents (Chen et al., 2017), toluene (Ma et al., 2022) or dyes such as methylene blue (Santos et al., 2020) by regenerating them with n. Other authors propose the adsorption of iron over the activated carbon surface as a previous step to the adsorption process of contaminants (Cabrera-Codony et al., 2015; Huling Scott et al., 2000; Huling and Hwang, 2010; Plakas and Karabelas, 2016) regenerating the spent carbon in batch by putting it in contact with a solution of H_2O_2.

Hydrogen peroxide presents promising results in recovering spent active carbon after the adsorption of pollutants from streams without surfactants. Even though some works have studied the adsorption of surfactants (Basar et al., 2004; Bautista-Toledo et al., 2008; Siyal et al., 2020) or emulsions with organic compounds (Ahn et al., 2007; Ahn et al., 2008b; Rosas et al., 2013; Yang et al., 2009; Zheng et al., 2018), the regeneration of spent carbon after adsorption of HOCs on emulsions.

To fill this gap, in this work, a two-step process technology has been validated using the emulsion generated in the SEAR process applied in the remediation of a highly polluted landfill with a DNAPL generated from the wastes of the production of the pesticide lindane (γ-hexachlorocyclohexane, γ-HCH) and composed of 28 chlorinated organic compounds (COCs), ranging from chlorobenzene to heptachlorocyclohexane (Santos et al., 2018). The SEAR process was carried out within the LIFE SURFING project (https://lifesurfing.eu/) in Sabiñanigo, Spain, using *E*-Mulse 3® (E3, EthicalChem) as a surfactant.

The two-step process was carried out in a fixed bed column of a commercial GAC used in the wastewater treatment plant at the Sabiñánigo landfill, previously treated to fix iron on its surface. In the first step, the emulsion is fed to promote the selective adsorption of COCs, obtaining an aqueous solution of surfactant without pollutants, which can be reused in the SEAR application. The second step was designed to regenerate the fixed bed column by removing the COCs from the GAC. The iron immobilized acted as a heterogeneous catalyst in the Fenton reaction, with hydrogen peroxide used to oxidize the COCs adsorbed, recovering the adsorption capacity of the GAC. The regenerated GAC is then ready to be used again in the first step.

The correct design is challenging to be a continuous process, which means that the emulsion can be continuously fed to the column, and the GAC can be continuously regenerated. This results in a more efficient and cost-effective process for treating emulsions. The novelty of this work is that the operation conditions are systematically studied to propose kinetics and equilibrium of the adsorption of COCs and a surfactant model capable of explaining the experimental results. The reaction between GAC and hydrogen peroxide in column mode was investigated to study the gas generation and temperature increase. After that, the adsorption in the column and the regeneration using hydrogen peroxide were applied in multiple adsorption and regeneration cycles to treat the SEAR application emulsion, validating the proposed technology, reducing the environmental impact, increasing the circular economy of the process and reducing the mass of wasted adsorbent.

2. Experimental section

2.1. Materials

DNAPL was obtained from Bailin landfill (Sabiñanigo, Spain) and was provided by the Government of Aragon (Spain). The DNAPL is composed of 28 COCs, being the Lindane (γ-hexachlorocyclohexane, γ-HCH) one of them. In Table SM1, the mass and molar concentration of the COCs in the aqueous emulsion, which are lumped as the sum of isomers of chlorobenzene (CB), dichlorobenzenes (DCB), trichlorobenzenes (TCB), tetrachlorobenzenes (TTCB), pentachlorocyclohexenes (PCX), hexaclorocyclohexanes (HCH), hexachlorocyclohexanes (HCX) and heptachlorocyclohexanes (HeCH), are given.

The surfactant selected for this study was *E*-Mulse® 3 (E3). E3 was selected for use in the SEAR process within the LIFE SURFING project (https://lifesurfing.eu/) in Sabiñanigo, Spain. The surfactant presented good results in the solubilization and mobilization of the DNAPL adsorbed in soil in the landfill. Besides, this surfactant is a non-ionic polyethoxylated, nontoxic, and biodegradable surfactant. The different emulsions were prepared, dissolving in 1 L of Milli-Q water and stirring the solution for 10 min. Subsequently, the DNAPL was added to the E3 solution (COCs: from 0 to 9.1 $g{\cdot}L^{-1}$), and the mixture was agitated for 24 h to ensure stable emulsion formation. The emulsion was settled for 1 h to allow precipitation of soil particles contained in the DNAPL (such as absorbed clays). The mass of COCs in DNAPL was 91 % of the DNAPL added. The concentration of COCs and surfactant used were aligned with the concentration of the emulsion obtained after the SEAR process of the LIFE SURFING process.

The Aragon Government supplied the GAC. The GAC was also used in the physicochemical water treatment plant of the Bailin landfill. Their properties were described elsewhere (Sánchez-Yepes et al., 2022; Sánchez-Yepes et al., 2023).Hydrogen peroxide (35 % *v*/v H_2O_2) was used as the oxidizing agent, and iron (II) was used as the catalyst from a sulfate heptahydrate ($FeSO_4{\cdot}7H_2O$, 99 %). Titanium (IV) oxysulfate (Sigma-Aldrich) was used to quantify H_2O_2. Ion chromatography uses sodium carbonate, sodium bicarbonate, sulfuric acid, and acetone (analytical reagent grade and supplied by Sigma-Aldrich.) to determine chloride and short-chain organic acid concentrations.

2.2. Procedure

Two sets of experiments were conducted to design the treatment of adsorption and regeneration of emulsions. In the first set (SET-A), the kinetic and isotherms adsorption of COCs and surfactants were studied in batch mode. In the second set (SET—B), different experiments were carried out in column mode to study the reaction between the GAC and the oxidant, the adsorption of emulsion step and the adsorbent regeneration in several cycles. The experimental conditions are summarized in Table SM2.

2.2.1. Batch experiments (SET-A). Adsorption kinetics and isotherms on pretreated GAC

The selective adsorption of COCs and E3 was studied in batch using a pretreated GAC with 12 $mg_{Fe(II)}\cdot g^{-1}$ of iron adsorbed. The adsorption kinetic was studied in runs at 20°C using different emulsions composed of 6 and 12 $g\cdot L^{-1}$ of E3 and different COCs concentration (0 to 9.1 $g\cdot L^{-1}$ of COCs). The emulsions were put in contact with 50 $g\cdot L^{-1}$ of GAC in a glass reactor magnetically stirred at 500 rpm without head space. The GAC was located inside a stainless-steel mesh to avoid the GAC abrasion generated by the agitation. 0.25 mL of aqueous samples were collected at different times during 168 h. The amount of E3 and COCs adsorbed at different reaction samples was calculated using Eq. (1).

$$q_j = \left(C_{j,0} - C_{j,t}\right)\cdot\frac{V_{Emulsion}}{W_{GAC}} \quad (j = E3, COCs) \tag{1}$$

being q_j ($mg_j\cdot g_{GAC}^{-1}$) the amount of E3 or COCs adsorbed on the carbon, $C_{j,0}$ and $C_{j,t}$ ($mg_j\cdot L^{-1}$) were the initial and over time E3 or COCs concentrations in solution, $V_{Emulsion}$ (L) denoted the volume of the emulsion, assuming the volume of the total samples taken is lower than 2 %. w_{GAC} (g) was the mass of GAC.

Conversely, the adsorption isotherms of E3 and COCs using a pretreated GAC with 12 $mg_{Fe(II)}\cdot g^{-1}$, at 20 °C and using emulsions composed of 6 and 12 $g\cdot L^{-1}$ of E3 and different COCs concentrations (0 to 9.1 $g\cdot L^{-1}$ of COCs). These experiments were conducted in a batch glass reactor containing 125 mL of emulsion without head space and different amounts of GAC placed in a stainless-steel mesh, with a concentration range within 0.1–50 $g_{GAC}\cdot L^{-1}$. After 168 h of agitation, the composition of the aqueous phase was analysed, and the adsorbed COCs and surfactant on GAC were calculated with the corresponding mass balances described in Eq. (1). All the experiments were conducted in triplicate, and the average values were subsequently employed in the results section.

2.2.2. Column experiments (set—B)

2.2.2.1. Column preparation and GAC pretreatment and Iron adsorption. 118 mm long glass columns with an internal diameter of 28 mm were used. The connections for the material inlet and outlet were placed at the ends and opposite each other. The carbon bed consists of 20 g of GAC located at the centre of the column. The carbon bed was 50 mm long and 28 mm in diameter. The GAC was placed between two stainless steel wire meshes to contain it, and the spaces between the bed and the column outlet were filled with 5 mm diameter glass beads. The assembly was closed with a rubber cap. 6 columns were prepared for the experiments. A scheme of the column assembly is shown in Figure SM1.

The GAC in the columns was pretreated by flowing 1 L of acidified water (pH 2.5 adjusted with H_2SO_4) through the glass column without recirculation at a constant 2 $mL\cdot min^{-1}$ flow rate. Following the acid treatment, the column was rinsed with 100 mL of Milli-Q water to displace the acidified water.

Three columns were treated with an iron (II) sulfate solution of concentration 4 $g_{Fe(II)}\cdot L^{-1,}$ while the other three columns were treated with a solution of concentration 2 $g_{Fe(II)}\cdot L^{-1}$. Each 250 mL solution was prepared using iron (II) sulfate, Milli-Q water, and sulfuric acid to adjust the initial pH to 2.5. The prepared solutions were fed to each column at a constant 2 $mL\cdot min^{-1}$ flow rate. The outlet stream was recirculated to the feed tank to simulate a batch-mode operation. A scheme of the experimental setup is shown in Figure SM2. The recirculation and adsorption process continued until the iron concentration in the feed bottle remained constant.

Finally, the column was washed with 100 mL of acidified water (pH 2.5 adjusted with H_2SO_4) at the same flow rate to remove any remaining iron solution. The amount of adsorbed iron was determined by balancing the amount of iron in the initial, final, and wash water solutions, as described in Eq. (2).

$$\boldsymbol{q_j} = \frac{\boldsymbol{V_L}\cdot\left(\boldsymbol{C_{j,0}} - \boldsymbol{C_{j,f}}\right) - \boldsymbol{V_{WASH}}\cdot\boldsymbol{C_{j,WASH}}}{\boldsymbol{w_{COL}}} \quad (\boldsymbol{j}: \boldsymbol{E3}, \boldsymbol{COCs}, \boldsymbol{Fe}) \tag{2}$$

being Δq_j ($mg_j\cdot g_{GAC}^{-1}$) the amount of E3, Fe or COCs adsorbed on the carbon, $C_{j,0}$, $C_{j,f}$ and $C_{j,WASH}$ ($mg_j\cdot L^{-1}$) were the initial and final concentrations of E3, Fe or COCs and concentration in the wash volume, V_L and V_{WAS} (L) denoted the volume of the iron solution or emulsion and wash volume. w_{COL} (g) was the mass of carbon in the column.

Consumption of H_2O_2 by the GAC: The H_2O_2 consumption in the column was monitored using four (ensembled columns previously treated with the Fe (II) solution of 4 $g_{Fe(II)}\cdot L^{-1}$ and 2 $g_{Fe(II)}\cdot L^{-1}$ to replicate the experimental results). 500 mL solution of 40 $g\cdot L^{-1}H_2O_2$ at 20 °C. Two feed flow rates (2 or 10 $mL\cdot min^{-1}$) were studied without recirculation. The experimental conditions are described in Table SM2. The total liquid flow, peroxide concentration, pH, temperature, and Fe concentration were monitored at different reaction times at the column outlet. In addition, the gas flow was measured to monitor the amount of gases generated in the reaction and decomposition of the oxidant. The two replicated experiments were used to corroborate the adsorption of iron obtained.

The study of the consumption of H_2O_2 was completed by carrying out two extra experiments in batch mode using well-mix reactors containing 50 mL of 166 mM H_2O_2 (5.6 $g\cdot L^{-1}$) and 5 $g\cdot L^{-1}$ of carbon at natural pH. The effect of the temperature was studied at 40 and 80 °C. The experimental conditions are described in Table SM3.

2.2.2.2. Adsorption of COCs and E3 in GAC in column. The adsorption was performed by passing 1 L of emulsion (4 $g\cdot L^{-1}$ of E3 and 2 $g\cdot L^{-1}$ of COCs) through the COL-Fe column, at the different loads of iron, at a constant flow rate of 2 $mL\cdot min^{-1}$. The effluent from the column was recirculated to the fed tank for 144 h, as summarized in Figure SM2. COCs and E3 concentration in the bottle were measured over time. Under this experimental procedure, the adsorption of E3 and COCs was carried out at batch conditions. Once the concentration of E3 and COCs in the fed tank remained constant, the column was rinsed by feeding 200 mL of milli-Q water at 2 $mL\cdot min^{-1}$ without recirculation. The output stream was collected separately, and COCs and E3 concentrations in the wash volume were quantified. The final adsorbed COCs and E3 were calculated by Eq. (2).

2.3. Regeneration of waste GAC and adsorption/regeneration cycles

The spent carbon in the column bed with different iron concentration adsorbed (was regenerated by feeding 500 mL of an aqueous H_2O_2 solution (40 $g\cdot L^{-1}$) at 20 °C and at a flow rate of 2 $mL\cdot min^{-1}$, without recirculation. The column outlet was connected to a gas separator where the aqueous and gas phase were separated. The aqueous phase was collected, as summarized in Figure SM3. Aqueous samples were periodically taken from the column aqueous outlet, where the concentration of H_2O_2, iron leached, COCs, chloride, sulfate, short-chain acids, pH, TOC, and temperature were measured. Once the whole H_2O_2 solution volume was fed, the column was washed with 200 mL of Milli-Q at 2 $mL\cdot min^{-1}$ and 20 °C. The wash volume was collected and analysed.

After the regeneration, several adsorption-regeneration cycles were

carried out for the columns with different amounts of iron adsorbed. After the regeneration cycle, the carbon was saturated with a fresh emulsion, as was described above and the amount of compounds adsorbed were calculated with Eq. (2), but expressed as the increment adsorption amount between cycles (C and C + 1) as is shown in Eq. (3).

$$\Delta q_j = q_{j,c+1} - q_{j,C} \tag{3}$$

2.4. Analytical methods

The characterisation of the emulsion was carried out using various analytical techniques. The COCs in the emulsion and in the regeneration aqueous phases were quantified by gas chromatography (GC) and TOC quantified the surfactant.

2.4.1. Gas chromatography (GC)

GC analysis was performed using an Agilent 6890 GC system equipped with both a flame ionisation detector and an Electron Capture Detector. The column used was Agilent HP5-MSUI (19091S-433UI) $19091S433UI,\ 30\ m \times\ 0.25\ mm\ ID \times\ 0.25\ \mu m$. Two microlitres of the sample were injected using helium as the carrier gas with a flow rate of 2.9 $mL{\cdot}min^{-1}$. The GC injection port temperature was set at 250 °C and the oven was programmed to increase the temperature at a rate of 15 $^{\circ}C{\cdot}min^{-1}$ until 180 °C and then hold it constant for 15min. A split ratio of 10:1 was used for the analysis. The samples were diluted 1:10 with methanol before injection. Each sample was analysed in triplicate, and the average values were subsequently employed in the results section.

2.4.2. Total organic carbon (TOC) analysis

The concentration of E3 in the emulsion was quantified by TOC analysis after subtracting the TOC corresponding to the solubilized COCs in the emulsion and considering the carbon ratio of carbon per gram of E3 was established and validated in 0.58 $g_C{\cdot}g_{E3}^{-1}$ (García-Cervilla et al., 2020). TOC analysis was performed using a Shimadzu TOC-V CSH analyser. The analysis involved oxidative combustion of the sample at 714 °C with a CO_2 infrared detector for detection.

2.4.3. Colorimetric

The H_2O_2 concentration was determined by colorimetric. Each sample was reacted with titanium (IV) oxysulfate, and the colour change was measured by a 410 nm spectrophotometer (BOECO S-20 VIS).

2.4.4. Ion chromatography (IC)

Ionic organic by-products, such as carboxylic acids and chlorides, were measured by IC using a Metrohm 761 Compact IC system with anionic chemical suppression and a conductivity detector.

2.4.5. pH measurement

The pH of the sample was measured using a Basic 20-CRISON pH electrode.

2.4.6. Surface GAC (BET method)

From the N_2 isotherm, the surface area and pore volume were determined by applying the BET equation. The samples were outgassed at 150 °C for at least 8 h and the N_2 adsorption-desorption was measured at —196C with ASAP 2020 apparatus (Micromeritics).

3. Results and discussions

3.1. Batch experiments (set-A): adsorption isotherm and adsorption kinetics

The adsorption kinetics of emulsions with 6 and 12 $g{\cdot}L^{-1}$ E3 concentrations and varying COCs concentrations from 0 to 9.1 $g{\cdot}L^{-1}$ was studied. The concentrations of E3 and COCs in the aqueous emulsion were measured over time. The amount of E3 and COCs adsorbed on GAC with 12 $mg_{Fe(II)}{\cdot}g^{-1}$ was calculated with Eq. (1). The experimental results are plotted in Fig. 1.

In Fig. 1a, the adsorption of E3 is plotted, while the adsorption of COCs is shown in Fig. 1b. Comparing the results of Fig. 1a and Fig. 1b, it was observed that increasing the concentration of COCs in the emulsion reduces the adsorption of E3. The latter agrees with the assumption that COCs compete by the adsorption sites with E3.

The equilibrium concentrations of COCs and E3 obtained at different GAC doses using different concentration ratios of E3 and COCs are plotted in Fig. 2. These values were measured in the aqueous solution at 20 °C and after 168 h of contact. The selected time was motivated by the results presented in Fig. 1. As can be seen, this time was enough for an emulsion composed of 12 and 9.1 $g{\cdot}L^{-1}$ of E3 and COCs to reach the equilibrium.

In this system, composed of two absorbable components (surfactant and the COCs lumped as one only compound), the equilibrium loading of COCs ($q_{eq,COCs}$) depends not only on the concentration of COCs in the aqueous phase ($C_{eq,COCs}$) but also on the equilibrium concentrations of E3 (Worch, 2012). This fact was considered using the modified Langmuir isotherms in Eqs. (4) and (5) were considered. In these equations, it was assumed that the parameter related to the adsorbate–adsorbent interaction energy, $K_{m,i}$, is independent of the concentration of the other compound. However, as can be seen in Fig. 3, the monolayer adsorption capacity ($q_{m,E3}$) seems to be influenced by the other compound concentration (Rosas et al., 2013).

$$q_{e,E3} = \frac{q_{m,E3}}{1 + k_{COCs}{\cdot}C_{e,COCs}^{p_{COCs}}} \cdot \frac{K_{m,E3}{\cdot}C_{e,E3}}{1 + K_{m,E3}{\cdot}C_{E3}} \tag{4}$$

$$q_{e,COCs} = \frac{q_{m,COCs}}{1 + k_{E3}{\cdot}C_{e,E3}^{p_{E3}}} \cdot \frac{K_{m,COCs}{\cdot}C_{e,COCs}}{1 + K_{m,COCs}{\cdot}C_{e,COCs}} \tag{5}$$

Due to the simultaneous adsorption surfactant and COCs by the GAC, the isotherms for the pure components cannot be determined in this specific case. For this reason, mixed adsorption data were calculated for a given initial compositions. The concentration of all components at equilibrium conditions were measured as a function of the adsorbent dose, as indicated. The parameters of Eqs. (4) and (5) were determined, fitting the experimental data to these equations and the mass balances in Eq. (6) where the initial concentrations and doses are considered (Worch, 2012). The parameters are summarized in Table 1, and the parity plot shows the predicted and experimental values in Figure SM4. A good agreement between experimental and predicted data was found.

$$C_{e,j} = C_{0,j} - q_{e,j}{\cdot}\frac{W}{V_L} \tag{6}$$

The emulsion adsorption kinetic on GAC with 12 $mg_{Fe(II)}{\cdot}g^{-1}$ was modelled by the Empirical Approach (EA) (Islam et al., 2021) given in Eqs. (7) and (8). The driving force is the difference between the adsorbed compound at a time ($q_{e,j}$ $mg_j{\cdot}g_{GAC}^{-1}$) and the corresponding equilibrium value $q_{j,t}$ ($mg_j{\cdot}g_{GAC}^{-1}$) for the concentration of the compound in the solution at the considered time (C_{j_t} in $g_j{\cdot}L^{-1}$).

$$\frac{dq_{COCs,t}}{dt} = k_{a,COCs}{\cdot}\left(q_{e,COCs} - q_{COCs,t}\right)^{n_{COCs}} \tag{7}$$

$$\frac{dq_{E3,t}}{dt} = k_{a,E3}{\cdot}\left(q_{e,E3} - q_{E3,t}\right)^{n_{E3}} \tag{8}$$

The kinetic parameters of Eqs. (7) and (8) were fitted to the experimental data plotted in Fig. 1. The kinetic parameters $k_{a\,j}$ were estimated by nonlinear regression (Marquardt algorithm) coupled to the Runge-Kutta algorithm, and the estimated values are shown in Table 1. The profiles of E3 and COC with time, shown as lines in Fig. 1, have been predicted. The agreement between the experimental and predicted values validates the proposed adsorption kinetic model. As is shown, the Fig. 1.

The adsorption kinetic constant of COCs is higher than the E3. These

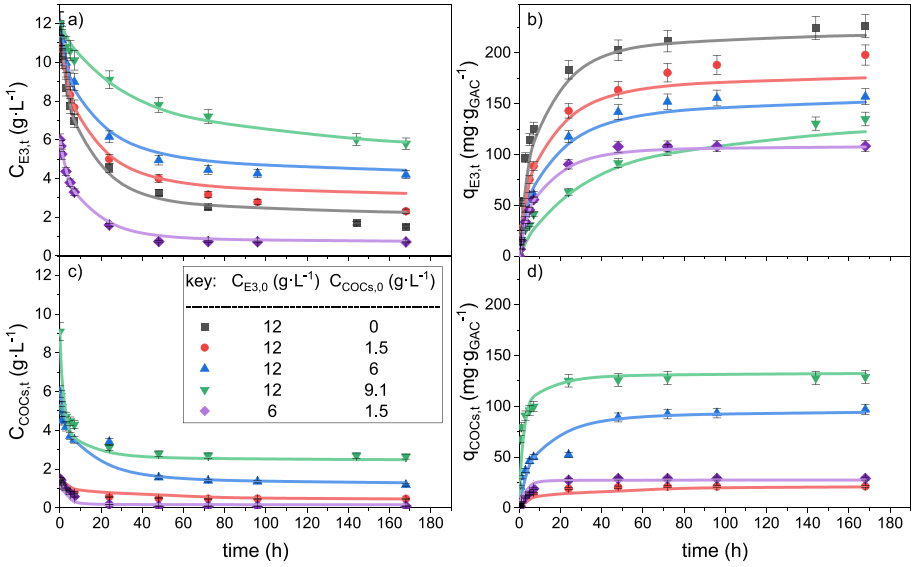

Fig. 1. Concentrations profile of a) E3 concentration in the aqueous emulsion b) E3 adsorbed in GAC c) COCs in aqueous in emulsion d) COCs adsorbed on GAC. $T = 20^{\circ}C$. $C_{E3,0} = 12\ g{\cdot}L^{-1}, C_{COCs,0} = 0 - 9.1\ g{\cdot}L^{-1}$ and $W_{GAC}{\cdot}V_{aq}^{-1} = 50\ g{\cdot}L^{-1}$. Symbols depict experimental values and lines corresponding to predicted values with the Eqs. (4) to (8)and the parameters in Table 1.

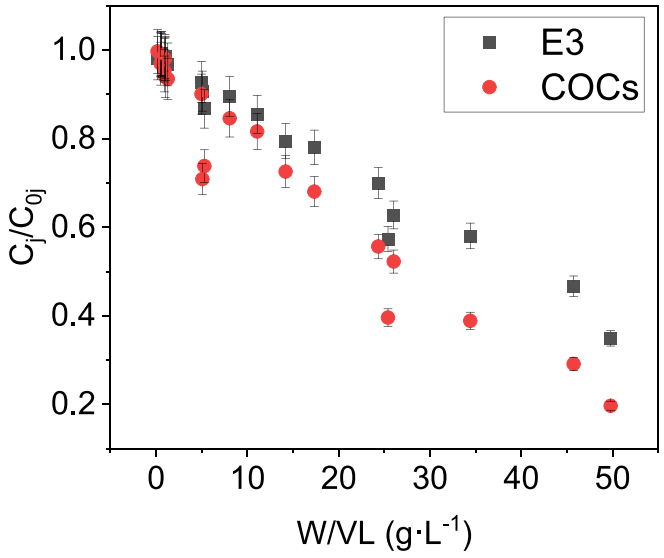

Fig. 2. The equilibrium concentration of E3 and COCs at different GAC doses. $C_{COCs,0} = 0 - 9.1\ g_{COCs}{\cdot}L^{-1}$ *and* $C_{E3,0} = 12 - 6\ g_{E3}{\cdot}L^{-1}$, $T = 20\ ^{\circ}C$.

results can be attributed to the increased hydrophobic nature of the COCs relative to E3, related to a higher partition coefficient for COCs compared to non-ionic surfactants (Ahn et al., 2007; Ahn et al., 2008a; Ahn et al., 2010a).

The selectivity of COCs adsorption can be quantified using Eq. (9) where the selectivity is calculated as the ratio of the reaction rates for COCs and E3 adsorption. This variable was calculated using the experimental data in Fig. 1, and the results are presented in Figure SM5. As seen in the time interval 0–10, the equilibrium condition was not reached, asserting that the adsorption rate for COCs is higher than that of E3.

$$S = \frac{dq_{COCs,t}}{dq_{E3,t}} = \frac{k_{a,COCs}{\cdot}\left(q_{e,COCs} - q_{COCs,t}\right)^{n_{COCs}}}{k_{a,E3}{\cdot}\left(q_{e,E3} - q_{E3,t}\right)^{n_{E3}}} \quad (9)$$

3.2. Column experiments (set—B)

3.2.1. GAC pretreatment

The adsorption of iron onto a granular activated carbon (GAC) column was investigated using initial concentrations of 2 and 4 g·L^{-1} of ferrous iron (Fe (II)) in an acidic aqueous solution. After 144 h of continuous recirculation and a subsequent acid water wash step, the amount of iron adsorbed onto the GAC was determined using Eq. (2). The results revealed that the columns treated with the 4 g·L^{-1} Fe (II) solution exhibited an iron adsorption capacity of 20 mg$_{Fe}$·g$_{GAC}^{-1}$ and a pH of 3.5 in the outlet stream, while those treated with the 2 g·L^{-1} Fe (II) solution displayed an adsorption capacity of 10 mg$_{Fe}$·g$_{GAC}^{-1}$ and a final pH of 2.7. These values represent the average of three replicates of the column experiments.

Comparing these results to those reported in previous work where the iron isotherm adsorption in GAC was obtained (Sánchez-Yepes et al., 2023), it was found that the adsorbed amount of Fe (II) onto the GAC when treated with 2 g·L^{-1} is consistent with the predicted value from the Langmuir isotherm. However, when the solution concentration was increased to 4 g·L^{-1}, the amount of iron retained in the column (20 mg$_{Fe}$·g$_{GAC}^{-1}$) exceeded the predicted value from the isotherm (12 mg$_{Fe}$·g$_{GAC}^{-1}$). The latter suggests that some iron was not effectively removed from the column during the acid water wash step.

The carbon pretreated was used to investigate the reaction between the GAC and H_2O_2. The experimental results of the oxidant reaction were obtained using 5 g·L^{-1} of carbon and a 166 mM H_2O_2 solution. The study was carried out at different temperatures (20–80 °C) to obtain the kinetic model of oxidant consumption. The experimental results are plotted in Figure SM6 and the kinetic parameters and the main conclusion are obtained in Text SM1.

The kinetic model proposed in Eq. SM2 was useful to predict the consumption of oxidant in column and the gas flow generated by this decomposition. The amount of gas generated can be a limitation of the column mode operation because the gas flow can produce an increment of the pressure inside the column putting in risk the normal column behaviour. The H_2O_2 consumption and gas production can be calculated in Eqs. SM3 and SM4 respectively, and plotted in Figure SM7, in function of temperature and W·Q$_L^{-1}$ (g·L^{-1} min^{-1}).

In Figure SM7, the predicted value of the gas flow was settled at 20 °C and using 2 and 10 mL·min^{-1} (W·Q$_L^{-1}$ = 1·10^{-4}, and 0.2·10^{-4}

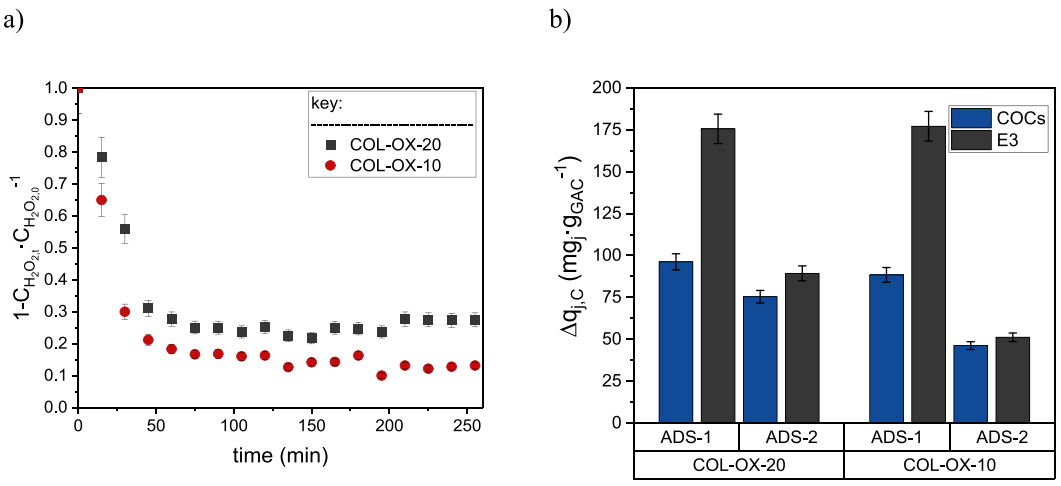

Fig. 3. a) H_2O_2 conversion at the column outlet with time as a function of the amount of adsorbed Fe. $C_{H2O2,0} = 40\ g{\cdot}L^{-1}$, $Q_L = 2\ mL{\cdot}min^{-1}$ and 20 °C. b) Increments of adsorbed COCs and E3. Initial emulsions contained $C_{COCs,0} = 2\ g{\cdot}L^{-1}$ and $C_{E3,0} = 4\ g{\cdot}L^{-1}$. The emulsion was recirculated for 144 h at a constant flow rate of 2 $mL{\cdot}min^{-1}$ and 20 °C.

Table 1
The parameters of the adsorption Langmuir isotherm are in Eqs. (4) and (5), and the kinetic parameters of the pseudo-second-order adsorption model are in Eqs. (7) and (8). Using GAC with 12 $mg_{Fe(II)}{\cdot}g^{-1}$ in Set-A.

	E3	COCs
Langmuir Isotherm. Eqs. (4) and (5)		
$q_{m,i}$ $\left(mg_i{\cdot}g_{GAC}^{-1}\right)$	242.03	291.81
$K_{m,i}$ $\left(L{\cdot}g_i^{-1}\right)$	1.74	1.04
k_i $\left(g_i{\cdot}L^{-1}\right)^{-p}$	3.63	0.21
p_i	−0.69	0.37
SQR[a]	836	863
Kinetic parameters. Eqs. (7) and (8).		
n_i	2	2
$k_{a,i}$ $\left(g_{GAC}{\cdot}mg_i^{-1}{\cdot}h^{-1}\right)$	$2.02{\cdot}10^{-4}$	$1.53{\cdot}10^{-3}$

[a] $SRQ = \sum \left(q_{e\,exp,j} - q_{e_{predicted,j}}\right)^2$ being $q_{e\,exp,j}\left(mg_j{\cdot}g_{GAC-W}^{-1}\right)$ and $q_{e\,predicted,j}\left(mg_j{\cdot}g_{GAC-W}^{-1}\right)$ the experimental and predicted adsorption capacity, respectively.

$g{\cdot}L^{-1}$ min^{-1}). Under these conditions the consumption of H_2O_2 was studied at column scale and using two loads of iron adsorbed (20 and 10 $mg{\cdot}g^{-1}$). The total gas flow, temperature, hydrogen peroxide, pH and Fe concentration in the outlet of the column were monitored over time. For those experiments carried out using a $W{\cdot}Q_L^{-1} = 1{\cdot}10^{-4}\ g{\cdot}L^{-1}\ min^{-1}$, the total consumption of hydrogen peroxide was observed, and the gas flow generated was 25 $mL{\cdot}min^{-1}$ according to the value predicted by the kinetic model for the experimental ratio. The concentration of adsorbed iron did not affect the consumption of hydrogen peroxide. Both columns (with 20 and 10 $mg{\cdot}g^{-1}$) obtained a consumption higher than 0.99 and an increase of 5 °C in the column temperature. On the contrary, with an increase in feed flow rate ($W{\cdot}Q_L^{-1} = 0.2{\cdot}10^{-4}\ g{\cdot}L^{-1}\ min^{-1}$) the consumption of hydrogen peroxide was reduced to 0.89 of the initials introduced to the column. As the feed flow rate increased (10 $mL{\cdot}min^{-1}$), so did the column temperature (up to 35 °C), resulting in a much higher gas yield, reaching 125 mL·min-1 values. The oxidation tests performed at a flow rate of 2 $mL{\cdot}min^{-1}$ generated a total loss of adsorbed iron less than 3 %.

The GAC treatment modified the original GAC, assuming a reduction of 18 %, from 851 to 702 $m^2{\cdot}g^{-1}$ with a variation in the pore volume of 0.380 to 0.309 $m^3{\cdot}g^{-1}$. This reduction in the area of BET was attributed to the fixation of the iron and oxidation of the GAC surface (Sánchez-Yepes et al., 2023).

3.2.2. Adsorption/regeneration process

The emulsion adsorption capacity of the GAC was studied in the column operation. Two different experiments were carried out using two columns with 20 $mg{\cdot}g^{-1}$ of iron adsorbed. One of those, COL-OX, was previously oxidated with 500 mL solution of H_2O_2 (40 $g{\cdot}L^{-1}$), flow rate of 2 $mL{\cdot}min^{-1}$ and 20 °C and raised with 100 mL of milli-Q water. The second adsorption experiments were conducted without the oxidation step named COL-NOX. In both experiments, an emulsion of $C_{COCs,0} = 2\ g{\cdot}L^{-1}$ and $C_{E3,0} = 4\ g{\cdot}L^{-1}$ was recirculated during 144 h. The amounts of E3 and COCs adsorbed were quantified using the balance described in Eq. (2). The concentration of Fe present in the final solution after adsorption was quantified, and the equivalent iron loss was calculated. The final values of concentration and equivalent loading of COCs and E3 were summarized in Table 2.

As shown in Table 2, there was no difference in the adsorption capacity of COCs and E3 in both experiments. However, the losses of the iron adsorbed were about 40 % of the initial iron trapped when the column was not previously oxidated. Iron fixed onto the GAC surface was 12.04 $mg{\cdot}g^{-1}$. This value agrees with the predicted by the adsorption isotherms using the GAC previously reported elsewhere (Sánchez-Yepes et al., 2023). The oxidation of GAC enhances the formation of oxidised groups that promote iron stability (Chen et al., 2007; Rey et al., 2009). For this, it was possible to fix the iron on the surface of the carbon, thus avoiding its loss in the following operations and obtaining Fe loads of 20 $mg{\cdot}g^{-1}$.

The adsorption capacity was also studied using those columns with 10 $mg{\cdot}g^{-1}$ of iron trapped previously oxidated to ensure the fixation of the metal. The amount of E3 and COCs adsorbed, and the losses of iron

Table 2
Amount of E3 and COCs adsorbed in columns with 20 $mg{\cdot}g^{-1}$ (COL-NOX-20 and COL-OX-20) and 10 $mg{\cdot}g^{-1}$ of iron (COL-OX-10). $C_{COCs,0} = 2\ g{\cdot}L^{-1}$ and $C_{E3,0} = 4\ g{\cdot}L^{-1}$ during 144 h at a constant flow rate of 2 $mL{\cdot}min^{-1}$ and 20 °C.

	q_{COCs} $\left(mg_{COCs}{\cdot}g_{GAC}^{-1}\right)$	q_{E3} $\left(mg_{E3}{\cdot}g_{GAC}^{-1}\right)$	% Fe
COL-NOX-20	82.95	172.83	39.8
COL-OX-20	96.20	175.56	1.10
COL-OX-10	88.42	177.12	0.81

are summarized in Table 2. The experimental results of experiments COL-OX-20 and COL-OX-10 showed no differences between the amounts of COCs and E3.

3.2.2.1. Regeneration. The columns with the pollutants adsorbed were used to test the regeneration of the GAC wasted, using COL-OX-20 and COL-OX-10 and the methodology described in the procedure section. In these regeneration steps, the outlet stream of the column was connected to a gas separator to monitor the flow of gas generated and the concentration of H_2O_2 in the liquid outlet.

The conversion of oxidant with time is plotted in Fig. 3 for both concentrations of iron in the GAC surface tested. As shown, the higher the iron content, the higher the conversion of oxidant since iron promotes hydroxyl radical generation (Pignatello et al., 2006). The conversion profiles were similar for both loads of iron. In an early stage, the conversion decreased for about 75 min, and then the conversion of the oxidant reached an asymptotic value. This trend can be explained by assuming that during the first 75 min, the oxidant was consumed in oxidating the COCs, and E3 adsorbed in the surface of the GAC. After, that consumption can be attributed to the unproductive consumption of H_2O_2. The iron losses in both experiments were lower than the 0.5 % of their initial iron adsorbed. In addition, the COCs desorbed resulted in a concentration of less than 10 $mg{\cdot}L^{-1}$, equivalent to a loss of less than 0.2 % of the initial amount of adsorbed COCs.

The regeneration of the GAC to restore its adsorption capacity for COCs was evaluated by feeding a fresh emulsion containing 4 $g{\cdot}L^{-1}$ of E3 and 2 $g{\cdot}L^{-1}$ of COCs and recirculating it for 144 h. The final concentrations of COCs and E3 were measured, and the equivalent loading on the column was calculated using Eq. (2). The experimental data are shown in Fig. 3b. As can be observed, both experiments commenced with comparable COCs and E3 adsorption levels. However, following the initial regeneration step, the quantity of COCs adsorbed on COL-OX-20 surpassed the adsorption observed on COL-OX-10. This observation aligns with the conclusion drawn from hydrogen peroxide consumption, suggesting that a higher iron concentration implies increased hydroxyl radical production and enhanced oxidation of the adsorbed compounds. For this reason, successful regeneration cycles were conducted with GAC containing 20 $mg{\cdot}g^{-1}$ of immobilized iron.

It was also worth mentioning that the regeneration process significantly reduced the adsorption of E3 (approximately halved, from 175 $mg_{E3}{\cdot}g^{-1}$ to less than 100 $mg_{E3}{\cdot}g^{-1}$). This suggests that the regenerated GAC can selectively adsorb COCs from a new emulsion and that lower surfactant adsorption leads to higher surfactant recovery in the final emulsion. This recovered E3 can be used for a new SEAR process.

The gas flow rates measured in the regeneration at the outlet of the COL-OX-20 and COL-OX-10 were 8.50 and 6.02 $mL{\cdot}min^{-1}$ respectively. Similarly, the theoretical O_2 flow rate obtained from the total H_2O_2 consumption (using Eq. SM(4)) was calculated. For COL-OX-20 the theoretical O_2 flow rate obtained was 8.29 $mL{\cdot}min^{-1}$ and 5.53 $mL{\cdot}min^{-1}$ for COL-OX-10. When comparing the measured flow rates with the theoretical ones, it can be observed that the O_2 flow rate is lower than the one measured in the regeneration, this is due to the fact that in the oxidative process other species such as CO_2 are generated. A big difference was observed between the flow rates obtained in the regeneration and in the study of the unproductive consumption, this was due to the fact that the presence of adsorbed compounds in the GAC reduced the surface of the carbon and therefore, the contact between the oxidant and the active centres with iron on the surface of the GAC.

3.2.2.2. Cycles of regeneration/adsorption steps. The circular economy principles require the GAC to be used in multiple regeneration/adsorption cycles. Two columns with 20 $mg{\cdot}g^{-1}$ of iron fixed by a previous oxidation step were used to carry out 4 regeneration steps and 5 adsorptions of emulsion composed of 4 $g{\cdot}L^{-1}$ of E3 and 2 $g{\cdot}L^{-1}$ of COCs. The experimental results are the average value of both columns used, finding a discrepancy between experimental results lower than 3 %.

The oxidant conversion at the outlet of the column for the four oxidative cycles is represented in Fig. 4, and the characterisation of the final aqueous volume of each cycle is summarized in Table 3.

In Fig. 4 the peroxide outlet concentration increased with the number of the regeneration cycle. For all cycles the maximum H_2O_2 consumption occurred in the first 100 min of the operation. The stationary unproductive consumption was lower with the cycle, ending with an outlet concentration value closed to the initial H_2O_2 fed in the final cycle. In Table 3 the total iron lost for the four regeneration cycles represented only a 3.44 % of the initial iron adsorbed. This value is considered as a minimal lost that would not invalidate the continuation of regenerative cycles. The total desorbed COCs aqueous concentration represented a value lower than 20 $mg{\cdot}L^{-1}$, which represents a loss of 1 % of the adsorbed COCs per cycle.

Ionic compounds were analysed and summarized in Table 3. Short-chain acid species such as acetic and formic acids were quantified. Low concentrations of chloride species were quantified. Less than 10 % of the chlorides were associated with the initially adsorbed COCs. This may be because low molecular weight chloride species may remain adsorbed on the carbon after regeneration, leaching as oxidation cycles are performed (Sánchez-Yepes et al., 2023). This phenomenon can be explained by observing that the concentration of chlorides increased in the aqueous volume collected with cycling.

The gas flow rates measured in the four regeneration cycles at the outlet of the COL-OX-20 columns and the theoretical O_2 flow rates obtained from the total H_2O_2 consumption (using Eq. SM(4)) are summarized in Table 3. As can be seen in Table 3, the total measured gas flow rates decreased with the regenerative cycles performed, so did the total oxidant consumption. In each cycle, the difference between the total gas flow rates and the theoretical O_2 flow rate was always less than 1 $mL{\cdot}min^{-1}$. This difference was due to the presence of other gases generated in the oxidation reaction of the adsorbed compounds in the GAC.

The recovery of the adsorption capacity of the GAC was evaluated with the adsorption of COCs and E3, which is the initial step of a subsequent regeneration. The experimental values are represented as bars in Fig. 5. The adsorption of adsorbed COCs was reduced in the first three cycles (down from 96.20 to 43.12 $mg_{COCs}{\cdot}g^{-1}$). From the third adsorption cycle onwards, adsorbed COCs stabilised at a value above 50 $mg_{COCs}{\cdot}g^{-1}$. In contrast, surfactant adsorption decreased with the regeneration cycles, inferring that the carbon adsorbed the chlorinated

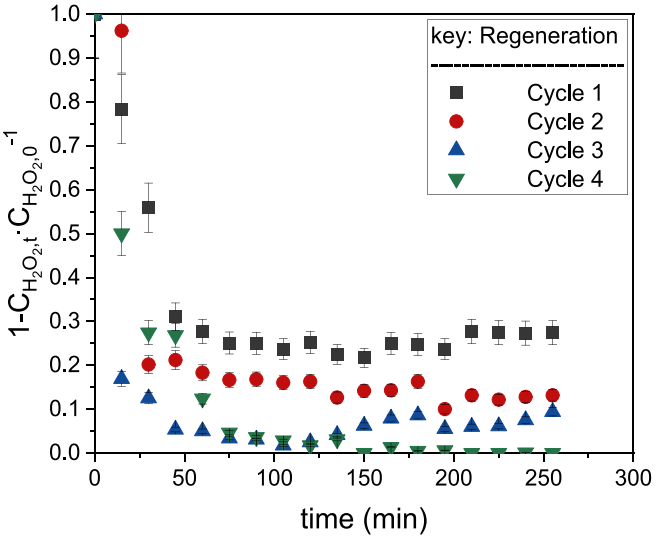

Fig. 4. H_2O_2 concentration at the column outlet with time in each regeneration cycle for COL-OX-20. The $C_{H2O2,0}$ = 40 $g{\cdot}L^{-1}$, Q_L = 2 $mL{\cdot}min^{-1}$ and 20 °C.

Table 3
Final concentrations in the aqueous regeneration phase. Iron lost by leaching ($mg_{Fe}\cdot g_{GAC}^{-1}$), chlorides ($Cl^-$) ($mg_j\cdot L^{-1}$), short-chain acids ($mg_j\cdot L^{-1}$) and COCs ($mg\cdot L^{-1}$). Measured gas flow rate at column outlet and theoretical O_2 flow rate generated from the total H_2O_2 decomposition (Q_{GAS}, $mL\cdot min^{-1}$). Results for the four regeneration cycles performed on the COL-OX-2 using the $C_{H2O2,0} = 40\ g\cdot L^{-1}$, $Q_L = 2\ mL\cdot min^{-1}$ and 20 °C.

Regeneration Cycle	% Fe	Cl^- ($mg\cdot L^{-1}$)	Short-chain ac. ($mg\cdot L^{-1}$)	COCs ($mg\cdot L^{-1}$)	Q_{GAS} ($mL\cdot min^{-1}$)	$Q_{O2,teorical}$ ($mL\cdot min^{-1}$)
1st	0.40	51.96	621.62	5.31	8.50	8.29
2nd	0.55	64.61	737.74	3.45	6.50	5.99
3rd	0.86	61.8	314.35	3.03	5.20	4.22
4th	1.63	97.29	396.88	6.95	5.50	4.08

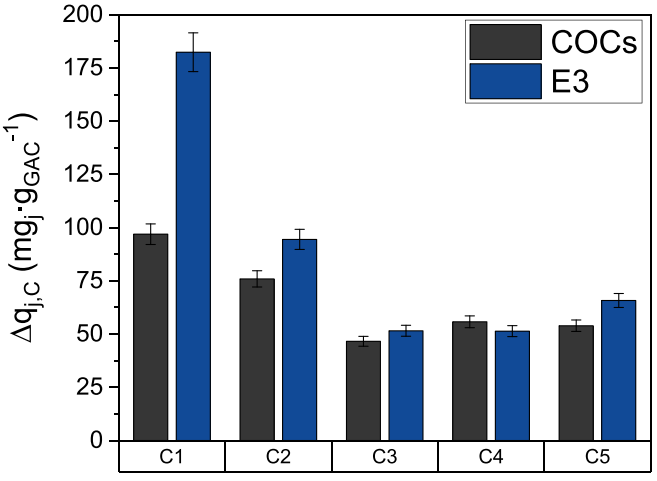

Fig. 5. Increments of adsorbed COCs and E3 in each adsorption cycle. Initial emulsions contained $C_{COCs,0} = 2\ g\cdot L^{-1}$ and $C_{E3,0} = 4\ g\cdot L^{-1}$. The emulsion was recirculated for 144 h at a constant flow rate of 2 $mL\cdot min^{-1}$ and 20 °C. Values after washing.

compounds from the emulsion selectively. The lower amount of adsorbed E3 resulted in a higher concentration of E3 recovered in the emulsion after adsorption.

The BET area at the end of the regeneration/adsorption cycles was measured, the surface area after 5 cycles using 20 $mg\cdot g^{-1}$ and 3 cycles using 10 $mg\cdot g^{-1}$ of iron were 63.1 and 58.6 $m^2\cdot g^{-1}$, and the pore volumes were 0.0325 and 0.0246 $m^3\cdot g^{-1}$, respectively. As can be seen, the surface BET decreased after the process, which can be related to a reduction in adsorption efficiency after each cycle.

4. Conclusions

A successful method was employed in a two-step process to treat a contaminated emulsion containing a non-ionic surfactant E3 and toxic COCs. The approach effectively managed on-site polluted emulsions, mainly from soil SEAR activities with highly toxic compounds. This method involved selectively adsorbing COCs onto GAC and regenerating spent GAC by oxidizing the adsorbed COCs with hydrogen peroxide. The iron previously fixed onto the GAC surface promoted the Fenton reaction. This reaction took place over the carbon surface since iron leaches were not produced thanks to the oxidation step of the carbon after the iron impregnation.

The preferential adsorption of COCs, is attributed to their higher hydrophobicity compared to E3. At the column scale, the recovery and reuse of surfactant and the reduction of organic compounds adsorbed onto GAC were achieved successfully after four cycles. During regeneration cycles, there was a notable reduction in oxidant consumption, primarily due to its efficient use in COC degradation. This approach reduced the amount of oxidant required for the treatment process. Furthermore, the aqueous phase obtained after each regeneration cycle exhibited lower toxicity than the initial polluted emulsion, with no toxic by-products from COC oxidation identified on the GAC surface. The findings support the potential of this technology for sustainable on-site management of contaminated emulsions resulting from SEAR application in soil remediation.

Nomenclature

Abbreviations

BET	Brunauer Emmett and Teller
CB	chlorobenzene
COCs	chlorinated organic compounds
DCB	dichlorobenzenes
DNAPLs	dense nonaqueous phase liquid
E3	*E*-Mulse-3®
GAC	granular activated carbon
GC	gas chromatography
HCH	hexaclorocyclohexanes
HCX	hexachlorocyclohexanes
HeCH	heptachlorocyclohexanes
HOCs	hydrophobic organic compounds
PCX	pentacyclohexenes
PVC	polyvinyl chloride
SEAR	surfactant-enhanced aquifer remediation
SM	supporting material
SRQ	sum of square residuals
TCB	trichlorobenzenes
TOC	total organic carbon
TTCB	tetrachlorobenzenes
SET-A	kinetic and isotherms adsorption experiments
SET-B	column experiments

Symbols

C_j	concentration of compound j, $mg\cdot L^{-1}$ *or* $g\cdot L^{-1}$
Ea/R	activated energy, K
k_i	kinetic adsorption constant, $L\cdot g^{-1}\cdot min^{-1}$
K_m	Langmuir adsorption constant
k_w	kinetic constant for H_2O_2 decomposition $L\cdot g^{-1}\cdot min^{-1}$
k_0	kinetic pre-exponencial constant for H_2O_2 decomposition $L\cdot g^{-1}\cdot min^{-1}$
$\overline{M_{COCs}}$	average molecular weights of COCs in the emulsion
M_j	molar concentration of compound j, $mmol\cdot L^{-1}$
M_W	molar mass of compound j, $mol\cdot g^{-1}$
n	kinetic adsorption order
q_j	amount of compound j adsorbed per unit mass of GAC $mg_j\cdot g_{GAC}^{-1}$
Q_L	volumetric flow, $L\cdot min^{-1}$
q_m	Langmuir maximum compound j adsorbed per unit mass of GAC $mg_j\cdot g_{GAC-W}^{-1}$
t	time
V_L	volume of the aqueous solution, L
w	mass of GAC, g
Δq_j	increase of the amount of compound j adsorbed per unit mass of GAC $mg_j\cdot g_{GAC}^{-1}$

X	convertion

Subindex

0	initial
e	equilibrium
exp	experimental value
f	final
j	compound
OUTLET	outlet of the column
predicted	predicted value
sample	sample
t	time
total	total
WASH	washes
bottle	bottle

CRediT authorship contribution statement

Andrés Sánchez-Yepes: Writing – review & editing, Writing – original draft, Methodology, Investigation, Formal analysis. **Aurora Santos:** Writing – review & editing, Writing – original draft, Supervision, Methodology, Investigation, Funding acquisition, Formal analysis, Data curation, Conceptualization. **Arturo Romero:** Writing – review & editing, Supervision, Investigation. **David Lorenzo:** Writing – review & editing, Writing – original draft, Supervision, Software, Methodology, Investigation, Formal analysis, Data curation, Conceptualization.

Declaration of competing interest

The authors declare that they have no known competing financial interests or personal relationships that could have appeared to influence the work reported in this paper.

Data availability

No data was used for the research described in the article.

Acknowledgements

This research is part of the project PID2022-137828OB-I00 (EMULREM) and PDC2022-133095-I00 funded by MCIN/AEI/10.13039/501100011033. This work was supported by the EU LIFE Program (LIFE17 ENV/ES/000260). A.S.-Y. would also like to thank the Ministry of Science and Innovation for supporting predoctoral contracts under FPI grant PRE2020-093195.

Appendix A. Supplementary data

Supplementary data to this article can be found online at https://doi.org/10.1016/j.scitotenv.2024.171847.

References

Ahn, C.K., Kim, Y.M., Woo, S.H., Park, J.M., 2007. Selective adsorption of phenanthrene dissolved in surfactant solution using activated carbon. Chemosphere 69, 1681–1688.
Ahn, C.K., Lee, M.W., Lee, D.S., Woo, S.H., Park, J.M., 2008a. Mathematical evaluation of activated carbon adsorption for surfactant recovery in a soil washing process. J. Hazard. Mater. 160, 13–19.
Ahn, C.K., Woo, S., Park, J., 2008b. Enhanced sorption of phenanthrene on activated carbon in surfactant solution. Carbon 46, 1401–1410.
Ahn, C.K., Woo, S.H., Park, J.M., 2010a. Selective adsorption of phenanthrene in nonionic-anionic surfactant mixtures using activated carbon. Chem. Eng. J. 158, 115–119.
Ahn, C.K., Woo, S.H., Park, J.M., 2010b. Selective adsorption of phenanthrene in nonionic–anionic surfactant mixtures using activated carbon. Chem. Eng. J. 158, 115–119.
Anfruns, A., Montes-Morán, M.A., Gonzalez-Olmos, R., Martin, M.J., 2013. H2O2-based oxidation processes for the regeneration of activated carbons saturated with volatile organic compounds of different polarity. Chemosphere 91, 48–54.
Basar, C.A., Karagunduz, A., Cakici, A., Keskinler, B., 2004. Removal of surfactants by powdered activated carbon and microfiltration. Water Res. 38, 2117–2124.
Bautista-Toledo, M.I., Méndez-Díaz, J.D., Sánchez-Polo, M., Rivera-Utrilla, J., Ferro-García, M.A., 2008. Adsorption of sodium dodecylbenzenesulfonate on activated carbons: effects of solution chemistry and presence of bacteria. J. Colloid Interface Sci. 317, 11–17.
Cabrera-Codony, A., Gonzalez-Olmos, R., Martín, M.J., 2015. Regeneration of siloxane-exhausted activated carbon by advanced oxidation processes. J. Hazard. Mater. 285, 501–508.
Cai, Q.Q., Wu, M.Y., Hu, L.M., Lee, B.C.Y., Ong, S.L., Wang, P., et al., 2020. Organics removal and in-situ granule activated carbon regeneration in FBR-Fenton/GAC process for reverse osmosis concentrate treatment. Water Res. 183, 116119.
Chen, Q., Liu, H., Yang, Z., Tan, D., 2017. Regeneration performance of spent granular activated carbon for tertiary treatment of dyeing wastewater by Fenton reagent and hydrogen peroxide. J. Mater. Cycles Waste Manag. 19, 256–264.
Chen, W., Parette, R., Zou, J., Cannon, F.S., Dempsey, B.A., 2007. Arsenic removal by iron-modified activated carbon. Water Res. 41, 1851–1858.
Fernández, J., Arjol, M.A., Cacho, C., 2013. POP-contaminated sites from HCH production in Sabiñánigo, Spain. Environ. Sci. Pollut. Res. Int. 20, 1937–1950.
García-Cervilla, R., Romero, A., Santos, A., Lorenzo, D., 2020. Surfactant-enhanced solubilization of chlorinated organic compounds contained in DNAPL from lindane waste: effect of surfactant type and pH. Int. J. Environ. Res. Public Health 17, 4494.
Huling, S.G., Hwang, S., 2010. Iron amendment and Fenton oxidation of MTBE-spent granular activated carbon. Water Res. 44, 2663–2671.
Huling, S.G., Ko, S., Park, S., Kan, E., 2011. Persulfate oxidation of MTBE- and chloroform-spent granular activated carbon. J. Hazard. Mater. 192, 1484–1490.
Huling Scott, G., Arnold Robert, G., Sierka Raymond, A., Jones Patrick, K., Fine, Dennis D., 2000. Contaminant adsorption and oxidation via Fenton reaction. J. Environ. Eng. 126, 595–600.
Huo, L., Liu, G., Yang, X., Ahmad, Z., Zhong, H., 2020a. Surfactant-enhanced aquifer remediation: mechanisms, influences, limitations and the countermeasures. Chemosphere 252, 126620.
Huo, L., Liu, G., Yang, X., Zhong, H., 2020b. Surfactant-enhanced aquifer remediation: mechanisms, influences, limitations and the countermeasures. Chemosphere 252, 126620.
Islam, M.A., Chowdhury, M.A., Mozumder, M.S.I., Uddin, M.T., 2021. Langmuir adsorption kinetics in liquid media: interface reaction model. ACS Omega 6, 14481–14492.
Jatta, S., Huang, S., Liang, C., 2019. A column study of persulfate chemical oxidative regeneration of toluene gas saturated activated carbon. Chem. Eng. J. 375, 122034.
Ma, L., Wu, Z., He, M., Wang, L., Yang, X., Wang, J., 2022. Experimental study on Fenton oxidation regeneration of adsorbed toluene saturated activated carbon. Environ. Pollut. 43, 524–533.
Panagos, P., Van Liedekerke, M., Yigini, Y., Montanarella, L., 2013. Contaminated sites in Europe: review of the current situation based on data collected through a European network. J. Environ. Public Health 2013, 158764.
Peng, J., Wu, E., Wang, N., Quan, X., Sun, M., Hu, Q., 2019. Removal of sulfonamide antibiotics from water by adsorption and persulfate oxidation process. J. Mol. Liq. 274, 632–638.
Pignatello, J.J., Oliveros, E., MacKay, A., 2006. Advanced oxidation processes for organic contaminant destruction based on the Fenton reaction and related chemistry. Crit. Rev. Environ. Sci. Technol. 36, 1–84.
Plakas, K., Karabelas, A., 2016. A Study on Heterogeneous Fenton Regeneration of Powdered Activated Carbon Impregnated With Iron Oxide Nanoparticles, Vol 18.
Rey, A., Faraldos, M., Casas, J.A., Zazo, J.A., Bahamonde, A., Rodríguez, J.J., 2009. Catalytic wet peroxide oxidation of phenol over Fe/AC catalysts: influence of iron precursor and activated carbon surface. Appl. Catal. B Environ. 86, 69–77.
Rosas, J.M., Santos, A., Romero, A., 2013. Soil-washing effluent treatment by selective adsorption of toxic organic contaminants on activated carbon. Water Air Soil Pollut. 224, 1506.
Sáez, P., Santos, A., García-Cervilla, R., Romero, A., Lorenzo, D., 2022. Non-ionic surfactant recovery in surfactant enhancement aquifer remediation effluent with chlorobenzenes by semivolatile chlorinated organic compounds volatilization. Int. J. Environ. Res. Public Health 19.
Sánchez-Yepes, A., Santos, A., Rosas, J.M., Rodríguez-Mirasol, J., Cordero, T., Lorenzo, D., 2022. Regeneration of granulated spent activated carbon with 1,2,4-trichlorobenzene using thermally activated persulfate. Ind. Eng. Chem. Res. 61, 9611–9620.
Sánchez-Yepes, A., Santos, A., Rosas, J.M., Rodríguez-Mirasol, J., Cordero, T., Lorenzo, D., 2023. Sustainable reuse of toxic spent granular activated carbon by heterogeneous Fenton reaction intensified by temperature changes. Chemosphere 341, 140047.
Santos, A., Fernández, J., Guadaño, J., Lorenzo, D., Romero, A., 2018. Chlorinated organic compounds in liquid wastes (DNAPL) from lindane production dumped in landfills in Sabiñanigo (Spain). Environ. Pollut. 242, 1616–1624.
Santos, D.H.S., Duarte, J.L.S., Tonholo, J., Meili, L., Zanta, C.L.P.S., 2020. Saturated activated carbon regeneration by UV-light, H2O2 and Fenton reaction. Sep. Purif. Technol. 250, 117112.
Seyedabbasi, M.A., Newell, C.J., Adamson, D.T., Sale, T.C., 2012. Relative contribution of DNAPL dissolution and matrix diffusion to the long-term persistence of chlorinated solvent source zones. J. Contam. Hydrol. 134-135, 69–81.

Shams, R., Alimohammadi, S., Yazdi, J., 2021. Optimizing surfactant-enhanced aquifer remediation based on Gaussian process surrogate model in DNAPL-contaminated sites considering different wells patterns. Groundw. Sustain. Dev. 15, 100675.
Siegrist, R.L., Crimi, M., Simpkin, T.J., 2011. In Situ Chemical Oxidation for Groundwater Remediation, Vol 3. Springer Science & Business Media.
Siyal, A.A., Shamsuddin, M.R., Low, A., Rabat, N.E., 2020. A review on recent developments in the adsorption of surfactants from wastewater. J. Environ. Manag. 254, 109797.
Toledo, L.C., Silva, A.C.B., Augusti, R., Lago, R.M., 2003. Application of Fenton's reagent to regenerate activated carbon saturated with organochloro compounds. Chemosphere 50, 1049–1054.
Trellu, C., Pechaud, Y., Oturan, N., Mousset, E., van Hullebusch, E.D., Huguenot, D., et al., 2021. Remediation of soils contaminated by hydrophobic organic compounds: how to recover extracting agents from soil washing solutions? J. Hazard. Mater. 404, 124137.
Worch, A.C.B.E., 2012. Berlin, Boston: De Gruyter.
Xiao, P.-f., An, L., Wu, D.-d., et al., 2020. New Carbon Mater. 35, 667–683.
Yang, J.-S., Baek, K., Kwon, T.-S., Yang, J.-W., 2009. Adsorption of chlorinated solvents in nonionic surfactant solutions with activated carbon in a fixed bed. J. Ind. Eng. Chem. 15, 777–779.
Zheng, X., Lin, H., Tao, Y., Zhang, H., 2018. Selective adsorption of phenanthrene dissolved in Tween 80 solution using activated carbon derived from walnut shells. Chemosphere 208, 951–959.